PMO_{12}@ZIF-8/ZnO Derived Hierarchical Porous Molybdenum Carbide as Efficient Electrocatalysts for Hydrogen Evolution

Jiao Li[†a], Xiao Li,[†*bc] Jing Sunbc, Xiaoli Hu [*bc] and Zhongmin Su [*bc]

[a]School of Materials science and Engineering, Changchun University of Science and Technology, Changchun 130022, People's Republic of China.

[b]School of Chemical and Environmental Engineering, Changchun University of Science and Technology, Changchun, People's Republic of China.

[c]Jilin Provincial Science and Technology Innovation Centre of Optical Materials and Chemistry, Changchun University of Science and Technology, Changchun, 130022, People's Republic of China.

E-mail: lix@cust.edu.cn, zmsu@nenu.edu.cn.

Experimental section

Chemicals

Zinc oxide (ZnO, Sinopharm Chemical Reagent Co., Ltd), 2-methyl imidazole (Jinan Henghua Sci. & Tec. Co., Ltd) and phosphomolybdic acid hydrate (Shanghai Xushuo Biological Technology Co., Ltd) were directly used without purification.

Synthesis of PMo_{12}@ZIF-8/ZnO

The synthesis procedure of PMo_{12}@ZIF-8/ZnO was according to the literature [1]. In detail, 5.0 mmol ZnO, 10.0 mmol 2-MeIM and 0.6 mmol $H_3PMo_{12}O_{40}\cdot xH_2O$ were successively put into the mill pot with 2 mL ethanol and mixed evenly. An appropriate amount of agate ball (10 mm) was added to the ball grinding tank, and the ball grinding was carried out at a speed of 40 Hz for 30 min. The resulting solid product was washed with large amounts of water and ethanol to remove excess polyacids and then dried at 60 ℃ for 12 h.

Synthesis of MoC@NC

Firstly, the PMo_{12}@ZIF-8 composite material was placed in a porcelain boat and heated to 900 ℃ for 2 h with the heating rate of 5 ℃ min^{-1} under Ar. Then, the obtained black powder was immersed in dilute hydrochloric acid and ultrasonic for 30 min. Finally, the samples are centrifuged and washed with a large amount of water until the solution

is neutral. The resulting samples were dried overnight at 80 ℃. In addition, a contrast sample of NC was synthesized by direct carbonization (900 ℃) without PMo_{12}.

characterizations

Powder X-ray diffraction (PXRD) patterns (Siemens D5005 diffractometer) were obtained by the Cu-Kα (λ=1.54118 Å) radiation with the 2θ of 5-80°. IR spectroscopy (Alpha Centaurt FT/IR spectrophotometer) was collected with the range of 4000-400 cm^{-1}. Transmission electron microscopy (TEM) images were measured via JEOL-2100F transmission electron microscope and SU8000 ESEM FEG energy dispersive X-ray detector (EDX). Raman spectra was gathered by the A JY Labram HR 800. The N_2 sorption tests (automatic volumetric adsorption equipment (Belsorp mini II)) were used to measure the surface area and pore volume of the catalyst. X-ray photoelectron spectroscopy (XPS) spectrums were obtained on a PHI Quantera SXM (ULVAC-PHI) with an Al Kα X-ray source.

Electrochemical measurements

All electrochemical tests were performed on a CHI 660e instrument with a traditional three-electrode system. In this work, glassy carbon electrode, graphite and Ag/AgCl electrode were used for working electrode, counter electrode and reference electrode respectively. 0.5 M H_2SO_4 and 1.0 M KOH solution were served as electrolyte for hydrogen evolution reaction (HER). 6.0 mg catalysts were dispersed in a mixture of 100 μL of 5 wt% naphthol, 200 μL of water and 200 μL of ethanol to form a homogeneous solution through ultrasound for 1 h. 5 μL of suspended liquid was dropped onto the glassy carbon electrode and the catalyst load was 0.85 mg cm^{-2}. Furthermore, the commercial Pt/C electrode was prepared in the same method.

The electrolyte was degassed with nitrogen before the polarization curve was measured. All potential reference reversible hydrogen electrodes were calculated using the Nernst equation: $E_{RHE} = E_{Ag/AgCl} + 0.059*pH + 0.197V$. Tafel plots were calculated by the equation of $\eta = a + b\log j$. Cyclic voltammetry (CV) was tested with the scan rates of 5, 10, 20, 50, 80 and 100 ranged from 0.1 to -0.1V. Electrochemical impedance spectroscopy (EIS) was measured at specific voltage and ranged from 0.1 to 100000 Hz. The stability was measured by chronoamperometry with *i*-t curves with a constant

working potential for 24 h in 0.5 M H_2SO_4 and 1.0 M KOH solutions respectively.

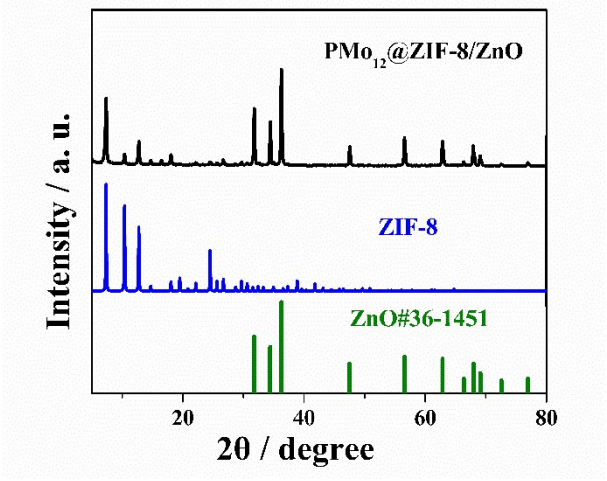

Figure S1. XRD patterns of PMo_{12}@ZIF-8 (Blue) and ZIF-8 simulated curves (Black).

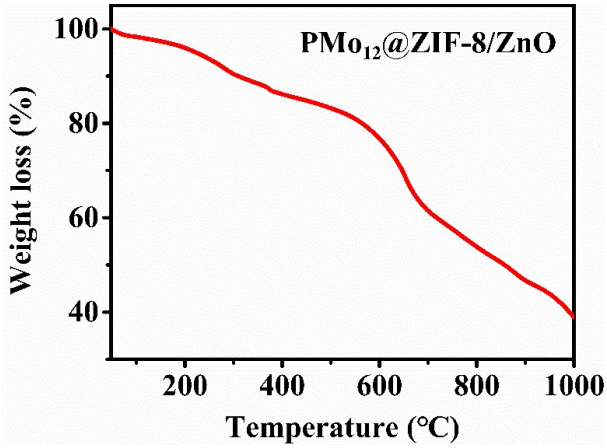

Figure S2. The TGA curves for PMo_{12}@ZIF-8/ZnO.

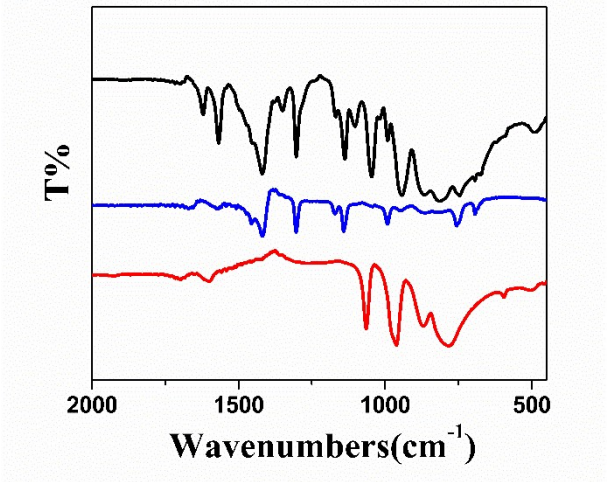

Figure S3. The IR spectrums of PMo_{12}@ZIF-8/ZnO (Black), ZIF-8 (Blue) and PMo_{12} (Red).

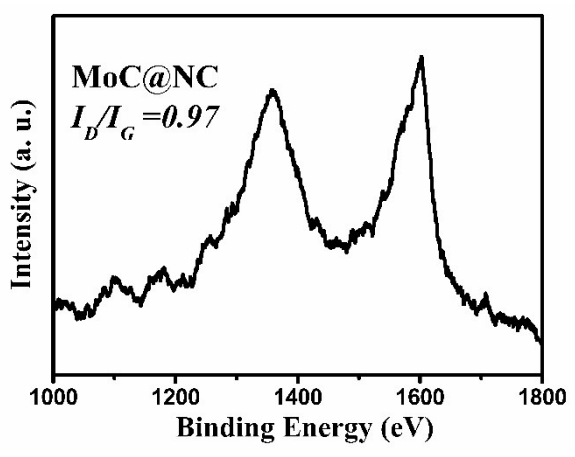

Figure S4. The Raman spectrum of **MoC@NC** with the carbonization temperature of 900 ℃.

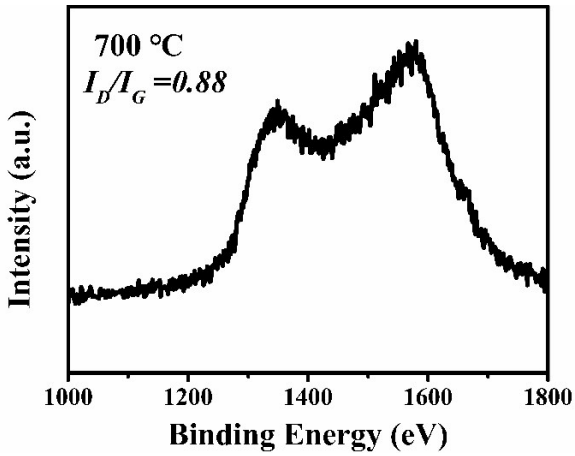

Figure S5. The Raman spectrum of **MoC@NC** with the carbonization temperature of 700 ℃.

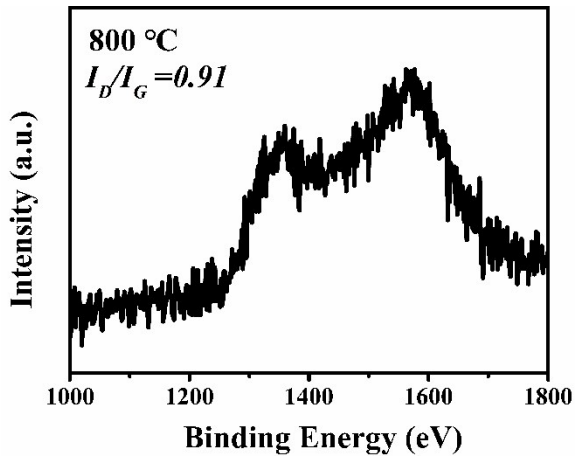

Figure S6. The Raman spectrum of **MoC@NC** with the carbonization temperature of 800 ℃.

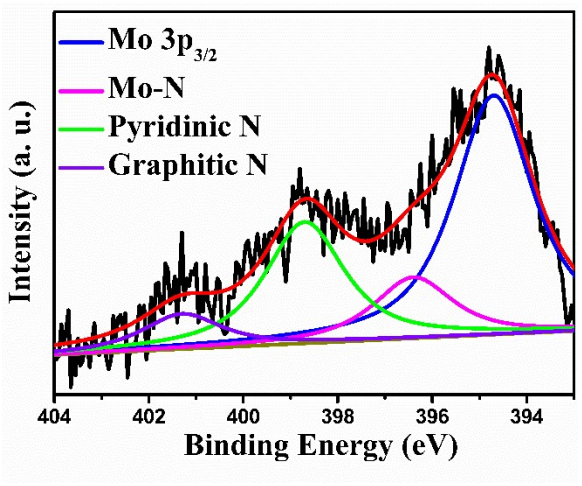

Figure S7. X-ray photoelectron spectroscopy (XPS) spectrums of N for **MoC@NC**.

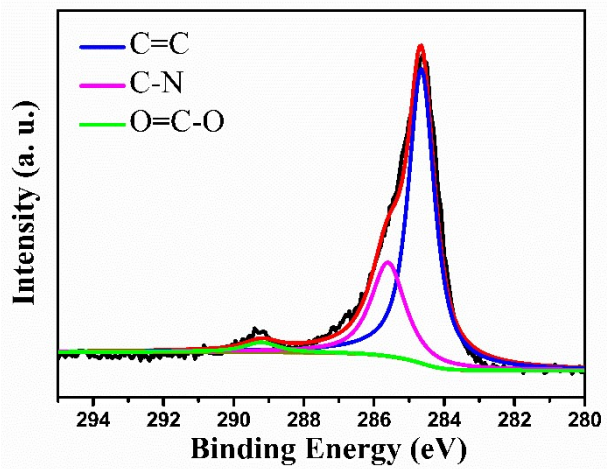

Figure S8. X-ray photoelectron spectroscopy (XPS) spectrums of C for **MoC@NC**.

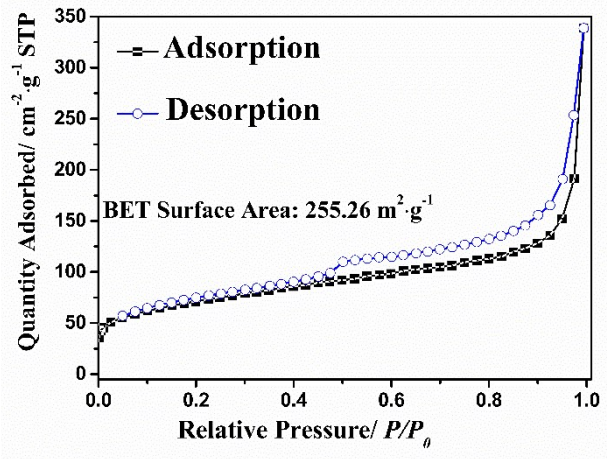

Figure S9. N_2 adsorption–desorption isotherms of **MoC@NC**.

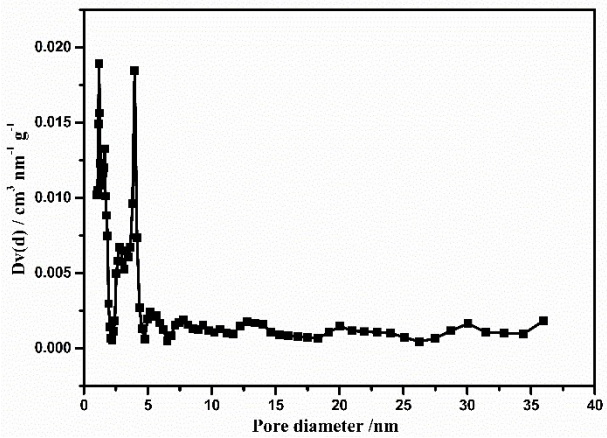

Figure S10. pore diameter distribution diagram of **MoC@NC**.

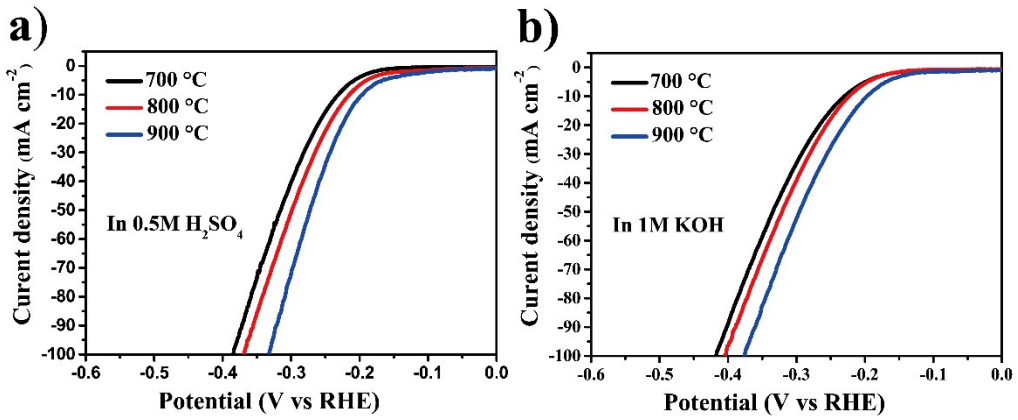

Figure S11. Polarization curves of **MoC@NC** obtained by carbonization for 2 h at different temperatures (700, 800 and 900 ℃), (a) acidic solution and (b) alkaline solution.

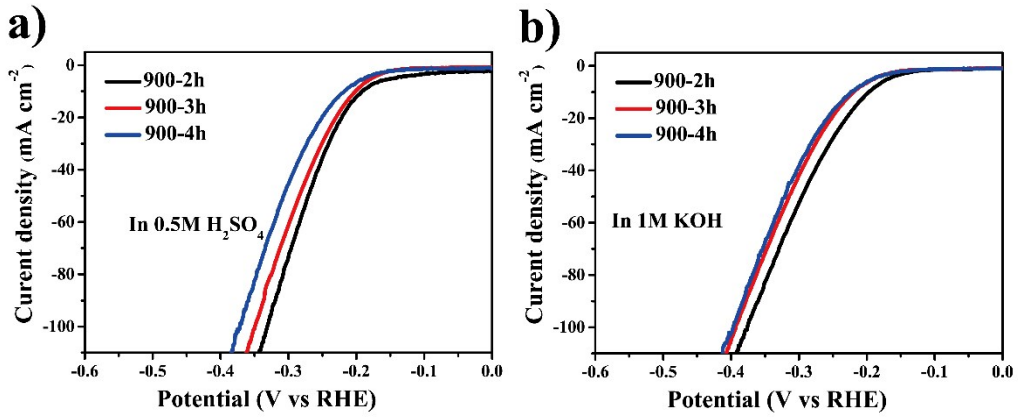

Figure S12. Polarization curves of **MoC@NC** obtained by carbonization at 900 ℃ with different times (2, 3 and 4 h), (a) acidic solution and (b) alkaline solution.

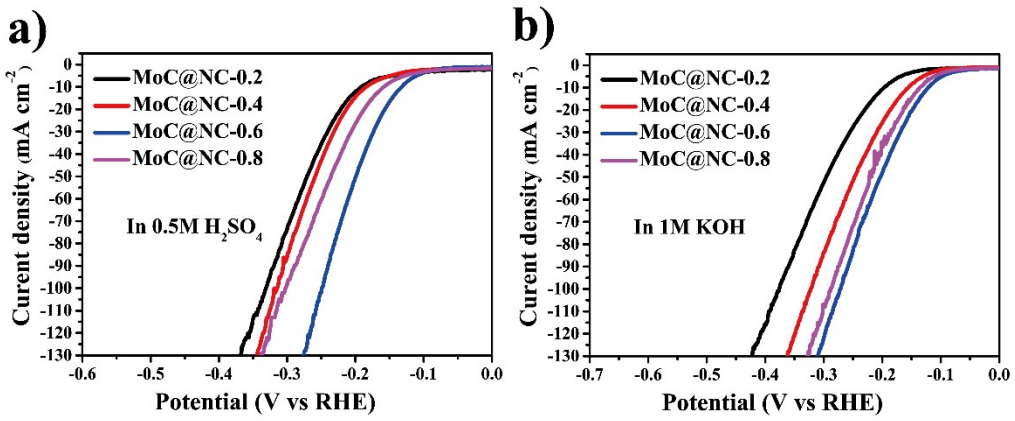

Figure S13. Polarization curves of **MoC@NC** obtained by different load (0.2, 0.4, 0.6 and 0.8 mmol), (a) acidic solution and (b) alkaline solution.

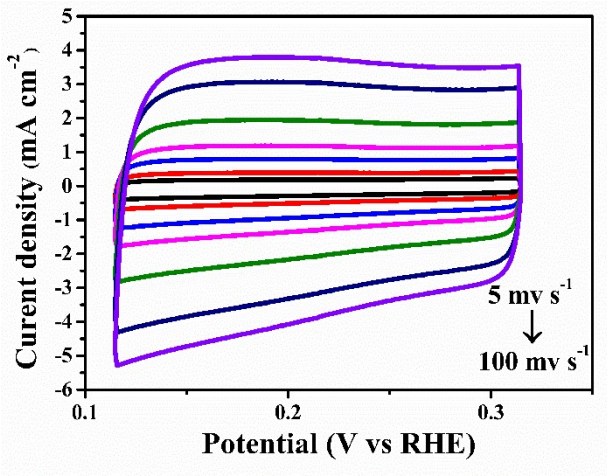

Figure S14. Cyclic voltammogram curves of **MoC@NC** at different sweeping speeds in 0.5 M H_2SO_4.

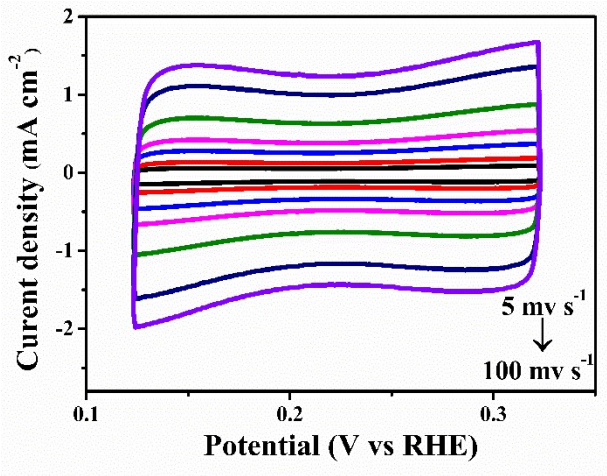

Figure S15. Cyclic voltammogram curves of **MoC@NC** at different sweeping speeds in 1.0 M

KOH.

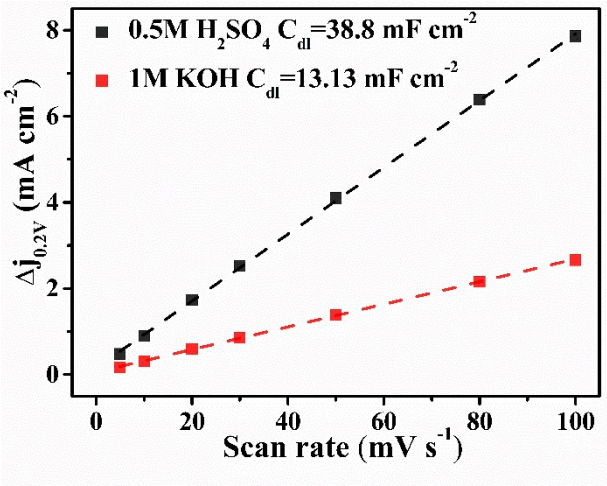

Figure S16. Double layer capacitance (C_{dl}) spectra of **MoC@NC** in 0.5 M H_2SO_4 and 1.0 M KOH.

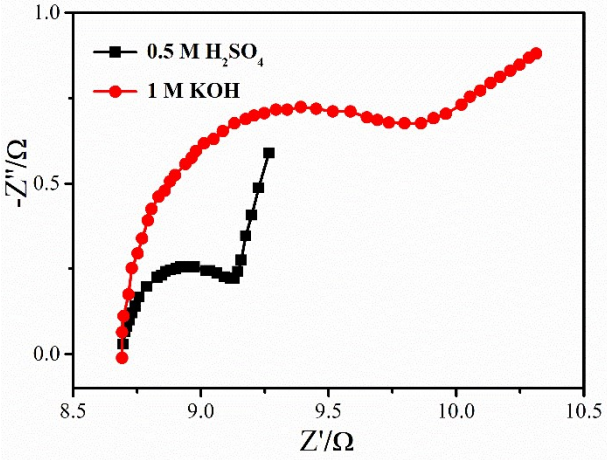

Figure S17. Nyquist plots of **MoC@NC** in 0.5 M H_2SO_4 and 1.0 M KOH.

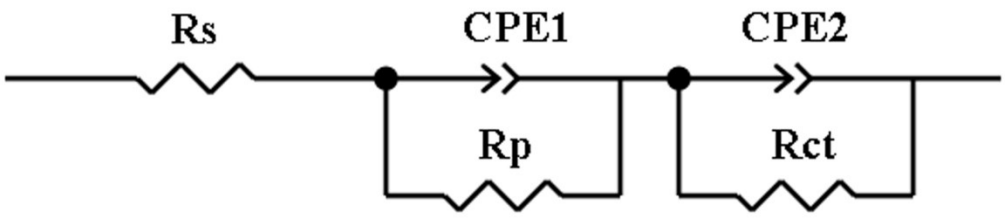

Figure S18. Fitting circuit diagram of **MoC@NC** in 0.5 M H_2SO_4 and 1.0 M KOH.

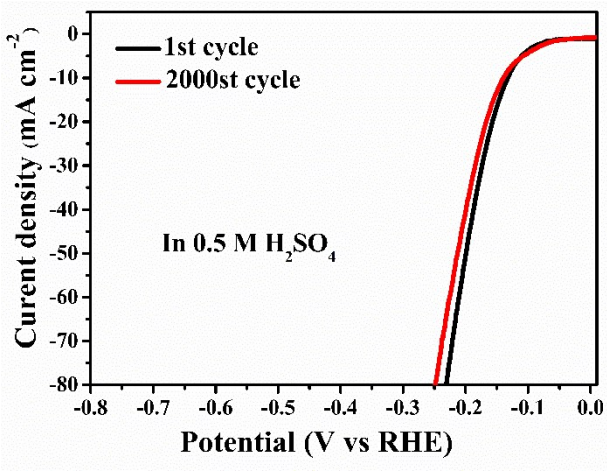

Figure S19. Polarization curves of **MoC@NC** before and after 2000 cycles in 0.5 M H_2SO_4.

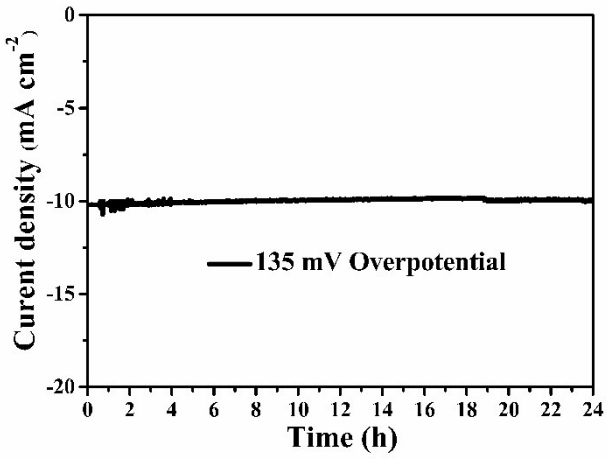

Figure S20. Time-dependent current density curve of **MoC@NC** in 0.5 M H_2SO_4.

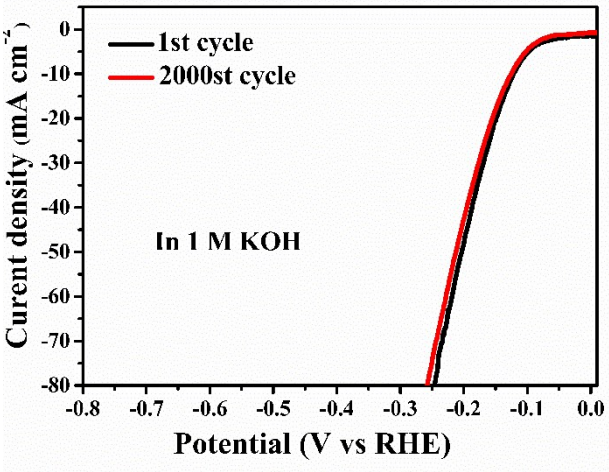

Figure S21. Polarization curves of **MoC@NC** before and after 2000 cycles in 1.0 M KOH.

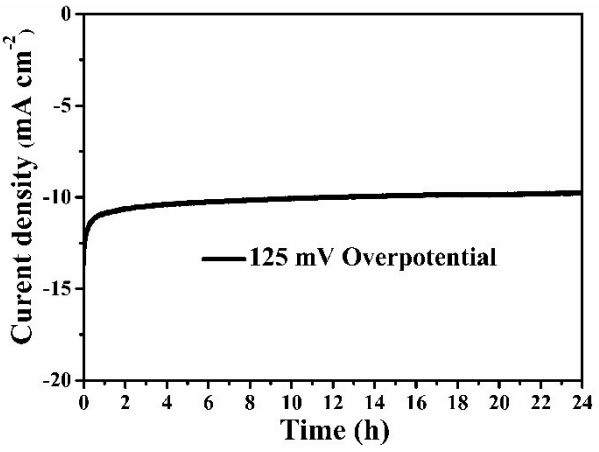

Figure S22. Time-dependent current density curve of **MoC@NC** in 1.0 M KOH.

Table S1. Element content values at different calcination temperatures.

Elements content (%)	**Mo**	**C**
700 ℃	50.620	20.340
800 ℃	52.580	17.570
900 ℃	55.350	15.730

Table S2. Comparison of HER performance of **MoC@NC** with other MoC-based HER catalysts.

Catalysts	Electrolyte	η_{10} (mV)	Tafel Slope (mV dec^{-1})	Stability	Ref.
MoC@NC	0.5 M H_2SO_4	132	75	24 h	This work
	1.0 M KOH	122	80	24 h	
Cu-Mo_xC_y	1.0 M KOH	190	51	1000 cycles	[2]
MoC-MoP/BCNC NFs	0.5 M H_2SO_4	158	58	24 h	[3]
	1.0 M KOH	137	65	24 h	
B-MoC	0.5 M H_2SO_4	285	128	8 h	[4]
MoC-Mo_2C	0.5 M H_2SO_4	126	43	3000 cycles	[5]
	1.0 M KOH	120	42	3000 cycles	
N,P-Mo_xC NF	0.5 M H_2SO_4	107	65.1	1000 cycles	[6]
	1.0 M KOH	135	57.1	1000 cycles	
N-Mo_xC@C HSs	0.5 M H_2SO_4	172	60	12 h	[7]
nanoMoC@GS	0.5 M H_2SO_4	124	43	10 h	[8]
	1.0 M KOH	77	50	-	
MoP/Mo_2C@C	0.5 M H_2SO_4	89	45	14 h	[9]
	1.0 M KOH	75	58	14 h	
	1.0 M PBS	136	93	14 h	
P-Mo_2C@NC	0.5 M H_2SO_4	109	76	12 h	[10]
	1.0 M PBS	159	-	12 h	
	1.0 M KOH	83	-	12 h	
Mo_2C-MoO_x/CC	1.0 M $HClO_4$	60	53	60	[11]

Reference

[1] Li R, Ren XQ, Zhao JS, Feng X, Jiang X, Fan XX, Lin ZG, Li XG, Hu CW, Wang B. Polyoxometallates trapped in a zeolitic imidazolate framework leading to high uptake and selectivity of bioactive molecules. J. Mater. Chem. A 2014;2:2168. https://doi.org/10.1039/C3TA14267A.

[2] Li P, Wu D, Dai C, Huang X, Li C, Yin Z, Zhou S, Lv Z, Cheng D, Zhu J. Controlled synthesis of copper-doped molybdenum carbide catalyst with enhanced activity and stability for hydrogen evolution reaction. Catalysis Letters 2019;149:1368–1374. https ://doi.org/10.1007/s1056 2-019-02695 -w.

[3] Chen NN, Mo Q, He L, Huang X, Yang L, Zeng J, Gao Q. Heterostructured MoC-MoP/N-doped carbon nanofibers as efficient electrocatalysts for hydrogen evolution reaction. Electrochimica Acta 2019;299:708-716. https://doi.org/10.1016/j.electacta.2019.01.054.

[4] Lin Q, Shang CQ, Chen ZH, Wang X, Zhou GF. Boron-doped molybdenum carbide as a pH-independent electrocatalyst for the hydrogen evolution reaction. International Journal of Hydrogen Energy 2020;45(55):30659-30665. https://doi.org/10.1016/j.ijhydene.2020.08.033.

[5] Lin HL, Shi ZP, He S, Yu X, Wang S, Gao QS, Tang Y. Heteronanowires of MoC–Mo_2C as efficient electrocatalysts for hydrogen evolution reaction. Chem. Sci 2016;7:3399. https://doi.org/10.1039/C6SC00077K.

[6] Ji L, Wang J, Xue T, Dong H, Chen Z. N,P-doped molybdenum carbide nanofibers for efficient hydrogen production. ACS Applied Materials & Interfaces 2018; 10(17):14632–14640. https://doi.org/10.1021/acsami.8b00363.

[7] Xiong TL, Jia J, Wei ZQ, Zeng LL, Deng YQ, Zhou WJ, Chen SW. N-doped carbon-wrapped MoxC heterophase sheets for high-efficiency electrochemical hydrogen production. Chemical Engineering Journal 2019;358:362-368. https://doi.org/10.1016/j.cej.2018.09.047.

[8] Shi ZP, Wang YX, Lin HL, Zhang HB, Shen MK, Xie SH, Zhang YH, Gao QS. Tang Y. Porous nanoMoC@graphite shell derived from a MOFs-directed strategy: an efficient electrocatalyst for the hydrogen evolution reaction. J. Mater. Chem. A 2016; 4:6006-6013. https://doi.org/10.1039/C6TA01900E.

[9] Zhang LN, Li SH, Tan HQ, Ullah Khan SF, Ma YY. MoP/Mo_2C@C: A new combination of electrocatalysts for highly Efficient hydrogen evolution over the entire pH range. ACS Appl. Mater. Interfaces 2017;9:16270−16279. https://doi.org/10.1021/acsami.7b03823.

[10] Yan G, Feng XJ, Ullah Khan SF, Xiao LG, Xi WG, Tan HQ, Ma YY, Zhang LN, Li YG. Polyoxometalate and resin-derived P-doped Mo_2C@N-doped carbon as a highly efficient hydrogen-evolution reaction catalyst at all pH values. Chem. Asian J 2018;13:158–163. https://doi.org/10.1002/asia.201701400

[11] He LQ, Zhang WB, Mo QJ, Huang WJ, Yang LC, Gao QS. Molybdenum carbide-oxide heterostructures: in situ surface reconfiguration toward efficient electrocatalytic hydrogen evolution. Angew. Chem. Int. Ed 2020;59:3544–3548. https://doi.org/10.1002/anie.201914752.